

INVESTIGATION OF THE INFLUENCE OF MAGNETIC ANOMALIES ON ION DISTRIBUTIONS AT MARS

H. NILSSON^{1,*}, E. CARLSSON^{1,2}, H. GUNELL¹, Y. FUTAANA¹, S. BARABASH¹,
R. LUNDIN¹, A. FEDOROV³, Y. SOOBIAH⁴, A. COATES⁴, M. FRÄNZ⁵
and E. ROUSSOS⁵

¹*Swedish Institute of Space Physics, P.O. Box 812, SE-981 28 Kiruna, Sweden*

²*Luleå University of Technology, Luleå, Sweden*

³*Centre d'Etude Spatiale des Rayonnements, Toulouse, France*

⁴*Mullard Space Science Lab, Imperial College, London, UK*

⁵*MPI für Sonnensystemforschung, Katlenberg-Lindau, Germany*

(*Author for correspondence, E-mail: hans.nilsson@irf.se)

(Received 7 May 2006; Accepted in final form 18 August 2006)

Abstract. Using data from the Mars Express Ion Mass Analyzer (IMA) we investigate the distribution of ion beams of planetary origin and search for an influence from Mars crustal magnetic anomalies. We have concentrated on ion beams observed inside the induced magnetosphere boundary (magnetic pile-up boundary). Some north-south asymmetry is seen in the data, but no longitudinal structure resembling that of the crustal anomalies. Comparing the occurrence rate of ion beams with magnetic field strength at 400 km altitude below the spacecraft (using statistical Mars Global Surveyor results) shows a decrease of the occurrence rate for modest (<40 nT) magnetic fields. Higher magnetic field regions (above 40 nT at 400 km) are sampled so seldom that the statistics are poor but the data is consistent with some ion outflow events being closely associated with the stronger anomalies. This ion flow does not significantly affect the overall distribution of ion beams around Mars.

Keywords: plasma, Mars, ions

1. Introduction

The solar wind interaction with the near-Mars space environment has been studied mainly by the Phobos-2 spacecraft [e.g. (Lundin *et al.*, 1989, 1991; Breus *et al.*, 1991; Barabash *et al.*, 1991; Trotignon *et al.*, 1996)], the Mars Global Surveyor (MGS) [e.g. (Mitchell *et al.*, 2000, 2001; Vignes *et al.*, 2000; Crider *et al.*, 2002; Krymskii *et al.*, 2003; Bertucci *et al.*, 2005; Brain *et al.*, 2005)], combinations of these two data sets (Trotignon *et al.*, 2006) and the, at the time of writing, most recently arrived spacecraft Mars Express [e.g. (Lundin *et al.*, 2004; Fränz *et al.*, 2005; Soobiah *et al.*, 2005)]. Much of the picture emerging from the first two spacecraft has been summarized in Nagy *et al.* (2004). The solar wind interaction with the near-Mars space results in several distinctive regions, mainly the bow-shock, the magnetosheath and the magnetic pile-up region. These regions are dominated by the solar wind magnetic field which is draped around the obstacle. However

MGS data shows clearly that the crustal magnetic fields [e.g. (Acuña *et al.*, 1998; Connerney *et al.*, 1999)] of Mars significantly affect the distribution of electrons in near-Mars space, in particular at the magnetic pile-up boundary (Vignes *et al.*, 2000; Crider *et al.*, 2002; Brain *et al.*, 2005) and the ionopause [e.g. (Mitchell *et al.*, 2001; Fränz *et al.*, 2005)].

The magnetic field of the magnetic pile-up region (MPR) is the interplanetary magnetic field draped around the planetary obstacle. The outer boundary towards the magnetosheath is termed the magnetic pile-up boundary (MPB) and is characterized from MGS measurements by an increase in magnetic field strength (Crider *et al.*, 2002) and a decrease in suprathermal electron fluxes and a decrease in magnetic field variability and wave activity (Brain *et al.*, 2005). The decrease in suprathermal electrons is consistent with energy loss of the magnetosheath electrons due to impact ionization of exospheric neutrals (Crider *et al.*, 2000). The MPB is thus not a pressure balance boundary, nor an impenetrable obstacle, at least not for magnetosheath electrons and magnetic fields. The ions of the magnetic pile-up region are expected to be mainly of planetary origin but the more extensive MGS data set lacks ion data.

The lower boundary of the magnetic pile-up region is characterized by a further reduction of the electron fluxes of magnetosheath origin, and below the MPR planetary origin photo-electron fluxes dominate. Mitchell *et al.* (2000, 2001) identify this as the Martian ionopause. The many strong crustal magnetic anomalies in the southern hemisphere stands off solar wind electrons up to higher altitudes in both the boundary regions.

The crustal magnetic fields also affect the ionosphere at altitudes well below the ionopause and even the neutral atmosphere. Krymskii *et al.* (2003) reported increased electron temperatures inside the “mini-magnetospheres” created by strong crustal magnetic fields, through confinement of photo-electrons, as well as a cooler neutral atmosphere which is shielded from additional heating by the solar wind interaction. Ness *et al.* (2000) reported an influence of magnetic fields on the ionospheric scale height, where horizontal fields inhibit vertical diffusion as compared to vertical or magnetic field-free regions. Mitchell *et al.* (2001) showed similar results at higher altitudes where strong crustal fields allowed the ionosphere to extend to higher altitudes, resulting in regions with enhanced photo-electron fluxes at an altitude of 400 km in the dayside. On the other hand photo-electron drift from day- to nightside and magnetosheath origin electron access were inhibited in the closed crustal fields on the nightside resulting in “void” regions with very low electron fluxes. Series of plasma void regions were often separated by electron flux-spikes. This tends to occur where the radial magnetic field is near a local maximum. The presence of magnetosheath-like electrons on such field-lines suggests that they are or were once connected to the magnetosheath, and the situation is thus similar to the cusps in the Earth’s magnetosphere but on a much smaller scale. Brain *et al.* (2006) took the similarities with the Earth further, showing that peaked electron spectra, resembling the accelerated electron spectra associated with aurora

on Earth, were frequently observed near strong radial crustal fields in the Martian nightside.

Thus the MGS results have firmly established the importance of the crustal fields for a number of electron plasma processes and structures at Mars. What about the influence of crustal fields on the ions? MGS lacks an ion spectrometer and we must now turn to Mars Express measurements.

We first tie the measurements from the two spacecraft together by looking at the reported electron observations from Mars Express. The work of Fränz *et al.* (2005) confirmed the crustal field influence on the statistical distribution of magnetosheath electron stand-off distance and the work of Soobiah *et al.* (2005) compared Mars Express electron spectrometer results with those obtained from MGS by Mitchell *et al.* (2001) and the Mars crustal magnetic field model of Cain *et al.* (2003) to investigate the influence of magnetic anomalies on the electron fluxes. They found that the presence of plasma voids in the nightside and flux enhancements in the dayside were well ordered by the Cain magnetic field model.

As Mars Express does not carry a magnetometer it is customary to call the planetary boundary towards the magnetosheath the Induced Magnetosphere Boundary (IMB) rather than the MPB, but it has been shown that on a large scale these are the same (Lundin *et al.*, 2004; Vignes *et al.*, 2000). The only works which so far have discussed ion observations in relation to magnetic anomalies are those by Lundin *et al.* (2004, 2005, 2006). These works report ion outflow as observed by the ASPERA-3 Ion Mass Analyzer (IMA). It is suggested that ion energization frequently involves acceleration by field-aligned electric fields and low frequency waves (as determined from electron flux variations, Winningham *et al.* (2005)). These can involve induced or draped magnetic fields just as well as crustal fields, but in Lundin *et al.* (2006) only deep nightside tail events were studied in an attempt to avoid the influence of non-crustal fields. Evidence of large scale field-aligned electric fields was found in the form of accelerated beam-like outflowing ionospheric ions observed simultaneously with precipitating electrons with peaked energy spectra, similar to what is observed in the auroral region on Earth. Mapping these events to crustal sources indicated that they were associated with magnetic cusps. The altitude of the observations was fairly high (several thousand km) and the mapping thus somewhat uncertain, but the association with magnetic anomalies is strengthened by the fact that the observations reported by Brain *et al.* (2006) clearly show that the peaked electron spectra observed by MGS at 400 km altitude are associated with strong radial crustal magnetic fields.

There thus seem to be cases when the magnetic anomalies may also be of importance for the ions. For the large scale distribution of ions this should mainly be for low energy ions or for field-aligned acceleration events because the crustal fields are relatively weak at altitudes where more energetic ions can be expected. The gyro-radii of ions quickly become large compared to the scale size of the anomalies when they are energized to energies observable by IMA (lower limit between 10 and 100 eV, see discussion in Section 2). However just as at Earth the

outflow of planetary ions is essentially a two-step process where the flow may either be regulated at the source (ionosphere, availability of ions) or by the energization process which typically occurs at higher altitudes. The purpose of this paper is to examine the potential role of crustal magnetic fields on the distribution of ions in near-Mars space. This has been done in 4 steps:

- (1) We have examined the clearest of the electron events reported by Soobiah *et al.* (2005) which were associated with magnetic anomalies and examined the corresponding ion data.
- (2) We have also examined the orbits containing the ion events used by Lundin *et al.* (2005) and compared the data with the Cain magnetic field model (Cain *et al.*, 2003) on a case basis.
- (3) We have studied the distribution of all energetic planetary ion beam events reported by Carlsson *et al.* (2006), including an extended study of similar events also for the year 2005.
- (4) We have gone through all the data when IMA was used in a non-entrance deflection scanning mode to improve time resolution and the ability to observe low energy ions (see Section 2).

2. Instrument Description

The Ion Mass Analyzer (IMA) is a mass resolving ion spectrometer, part of the ASPERA-3 instrument onboard Mars Express (Barabash and The ASPERA-4 Team, 2006). IMA's twin ICA on the Rosetta spacecraft is described in detail in Nilsson *et al.* (2006). IMA consists of an electrostatic acceptance angle filter, an electrostatic energy filter, and a magnetic velocity analyzer. Particles are detected using large diameter (100 mm) microchannel plates and a two-dimensional anode system. The energy range of the instrument is nominally from 10 eV to 36 keV and an angular field-of-view of $360^\circ \times 90^\circ$ is achieved through electrostatic deflection of incoming particles. This field of view is partially obstructed by the spacecraft body and the solar panels. IMA is mounted on the spacecraft $-Z$ side, facing towards spacecraft $-Y$ (i.e. the instrument symmetry axis is along spacecraft Y), see Figure 1. The basic field-of-view of the instrument is the spacecraft $X-Z$ plane, particles are brought in from $\pm 45^\circ$ out of this plane through the electrostatic deflection system. The deflection system does not have high enough voltage to reach all angles for the highest energies and not enough voltage resolution to reach all deflection angles for low energies. Above 15 keV the field-of-view is restricted towards the central viewing plane. For energies below 100 eV the angular resolution is degraded. Turning off the entrance deflection scan and using the instrument in a 2D mode removes the resolution problems at low energies and improves the instrument's ability to measure low energy ions as well as the time resolution. The time for one full energy scan is 12 s. and for one full measurement of 16 different

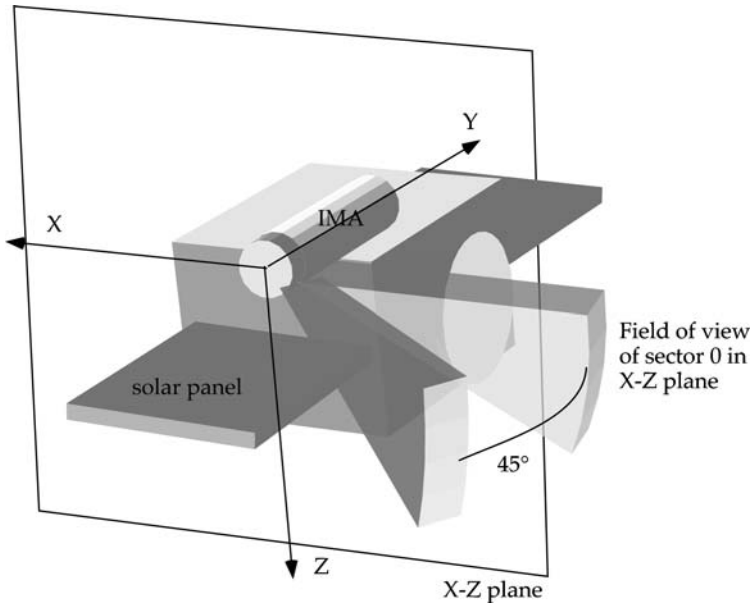


Figure 1. Schematic figure of the IMA Ion Mass Analyzer on the Mars Express spacecraft. Indicated are the spacecraft coordinate system and the field-of-view of one sector of the instrument at no deflection and at 45° away from the spacecraft.

deflection angles the time resolution becomes 192 s. The no entrance deflection mode may therefore be necessary to catch any finer structure of the ion distribution, in particular at low altitude where high time resolution is more important. IMA may run in different spatial and mass resolution modes to save telemetry. In practice almost all data is in the full resolution mode; no binning of data from different acceptance angles or binning of mass anodes is made (instrument mode 24).

Mass resolution is obtained through the magnetic velocity analyzer, where particles with the same energy but different mass will hit the micro-channel plate in different locations due to the analyzer magnetic field. The range of masses observable and the mass resolution can be influenced by adding energy to the incoming particles through a post-acceleration voltage. This voltage is applied between the electrostatic energy filter and the magnetic velocity analyzer and is controlled by a 3-bit reference value (0–7), corresponding to post-acceleration voltages between 0 and 4.3 kV.

3. Observations

3.1. ELECTRON EVENTS ASSOCIATED WITH MAGNETIC ANOMALIES

The clearest and most pronounced electron signatures associated with magnetic anomalies reported by Soobiah *et al.* (2005) were investigated to see if any ion signatures were found. This corresponded to 20 events selected from a total of 57

events identified in data from 144 orbits. The result was negative. Usually no ions at all were detected and when ions were detected they were not exactly coincident with either electron signatures or magnetic anomalies as determined from the Cain model (Cain *et al.*, 2003). Care was taken to determine that the IMA instrument was looking downward during at least some of the events. However the poor angular coverage at low energies means that there may still be low energy ions associated with the magnetic anomalies (there must be at least thermal ions due to charge neutrality).

3.2. MAGNETIC FIELDS AROUND CLEAR ION OBSERVATION EVENTS

Having failed to find good ion data in step 1 described above we proceeded to check the magnetic field as determined from the Cain model around some clear ion signatures, those reported by Lundin *et al.* (2005). A total of 30 events were plotted and investigated in detail. Typically ion beams were observed at the lowest altitude and some cases occurred at magnetic anomalies. However ion beams clearly existed even when no magnetic anomaly was nearby or the extrapolated Cain model field was very weak at the altitude of observation. No general similarity in the fine structure of ions and the magnetic field model was found though the temporal resolution may have been too poor to allow such a comparison. We report this part of the study for completeness, but will show data only from the cases when the IMA instrument was run in the “no entrance deflection” mode in Section 3.4). Then we also make a comparison with the magnetic field at a fixed altitude to avoid the risks inherent in extrapolating the Cain model to higher altitudes than the data from which the model was obtained.

3.3. THE DISTRIBUTION OF PLANETARY ORIGIN ION BEAM EVENTS

Here we used the data base of the ion observations used by Carlsson *et al.* (2006). It consists of all heavy ion beams (O^+ , CO_2^+ , CO^+/O_2^+) as identified from manual inspection of data from inside the nominal Induced Magnetosphere Boundary (IMB). A sample ion beam (in high time resolution “no entrance deflection mode”) is shown in Figure 2. The same event is marked with number 1 in Figure 7. The observation altitude was in the range 2000–3000 km, and the solar zenith angle was 136° – 140° .

This database has been updated with all ion beam events observed up to 22 October 2005, likewise determined from visual inspection of all IMA data obtained inside the nominal IMB. In Carlsson *et al.* (2006) only post-acceleration level 1 (out of three, 0 (none), 1 (reference value 1–4) and 2 (reference value 5–7)) was used, but for the subsequent data all identified events regardless of post-acceleration setting have been used (a total of 818 events). Before proceeding to investigate a possible influence on the distribution of planetary origin ion beams from crustal

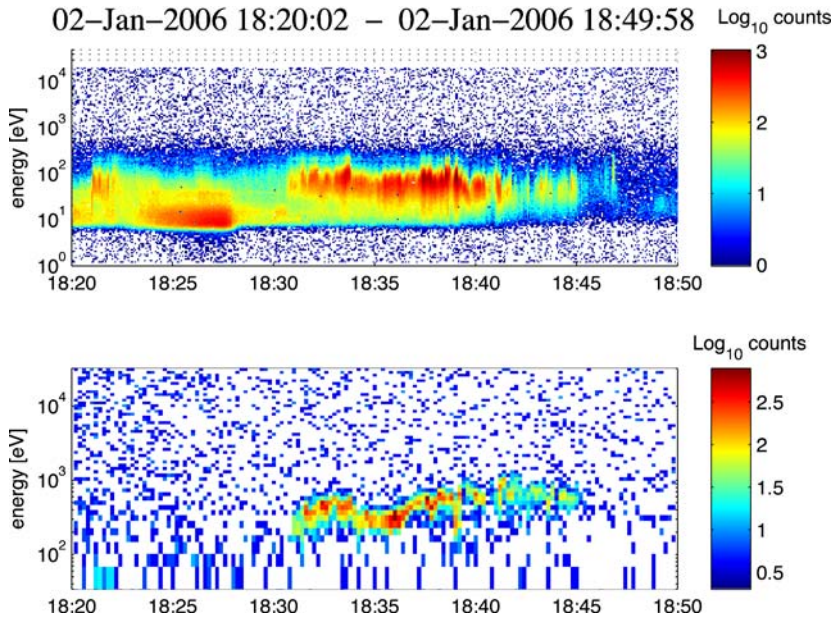


Figure 2. Sample energy spectra of a heavy ion beam from 20060102 when no entrance deflection scanning was used. The upper panel shows the corresponding electron spectra summed over all sectors (the electrons are typically rather isotropic). The lower panel shows the ion counts, summed over all sectors. One sector dominates and only a few sectors (of $22.5^\circ \times 5^\circ$) detect any ions at all. The Y-axis shows particle energy in eV for both panels, and the x-axis time (UT).

magnetic fields, we show in Figure 3 the ion beam occurrence rate (panel a) and the spacecraft coverage (number of passes in bin, panel b) as a function of solar zenith angle (x -axis) and altitude (y -axis). As can be seen, there is a clear dependence in the sense that dayside beams are observed at low altitude and nightside beams at high altitude. A lack of coverage at the lowest nightside altitudes is also evident, caused by restricted operation in spacecraft eclipse. Essentially the distribution follows what we expect from the induced magnetosphere boundaries and we can say that we do not have a strong dependence on solar zenith angle.

In order to search for an influence on the distribution of these ion beam events from magnetic anomalies, we have plotted their occurrence rate as a function of latitude and longitude, using 20×20 bins, i.e. a resolution of $18^\circ \times 9^\circ$ in longitude-latitude space. The data was also binned in altitude, and the normalized result for four different altitude bins (up to 1000 km, 1000–2000, 2000–3000 and 4000–10000 km) is shown in Figure 4. The distribution was calculated such that each “event” (continuous presence of an ion beam) was counted only once inside each latitude, longitude and altitude bin. The same type of distribution was then obtained for all cases when IMA was on in full resolution mode (mode number 24), post-acceleration setting was 1 for the 2004 data (all according to the housekeeping data) and Mars Express was inside the nominal IMB. This result was used to normalize

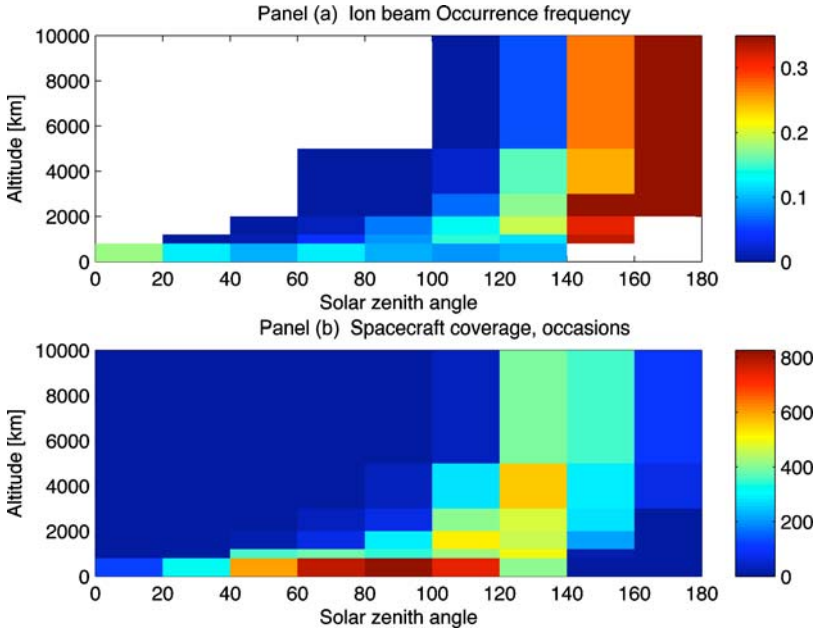


Figure 3. Panel (a) Distribution of occurrence rate of ions beams as a function of solar zenith angle (x -axis, degrees) and altitude (y -axis, [km]). Panel (b) Number of satellite passes through each statistical bin when IMA was operating in an appropriate mode.

the beam occurrence. What is shown in Figure 4 is the normalized occurrence frequency. The number of events is rather small and the plot in Figure 4 therefore rather noisy. It can nevertheless clearly be noted that the events occur over all locations on Mars. There seems to be some preference for northern latitudes for low altitudes (below 1000 km, panel a) and some preference for southern latitudes just below the equator at high altitude (above 3000 km, panel d). There is also a relatively low occurrence frequency for the southernmost latitude bins. Possibly this could indicate a large-scale influence from magnetic anomalies as these are stronger in the southern hemisphere. However latitude distributions are very sensitive to the orbit characteristics which causes an ambiguity between altitude and latitude dependence. The perigee is drifting so in due time all latitudes will be sampled at different altitudes but this is not true for a data set from a limited time interval such as the three-month data with entrance deflection turned off discussed in Section 3.4.

There is no longitudinal distribution (which is much less sensitive to orbit characteristics) resembling that of magnetic anomalies which are shown in Figure 7. To further investigate the significance of the observed north-south asymmetry we plot in Figure 5 the number of orbits when IMA was on in the right mode when Mars Express passed above the indicated latitude and longitude bin. Clearly there are a significant amount of samples in the south for low altitudes as well as for the

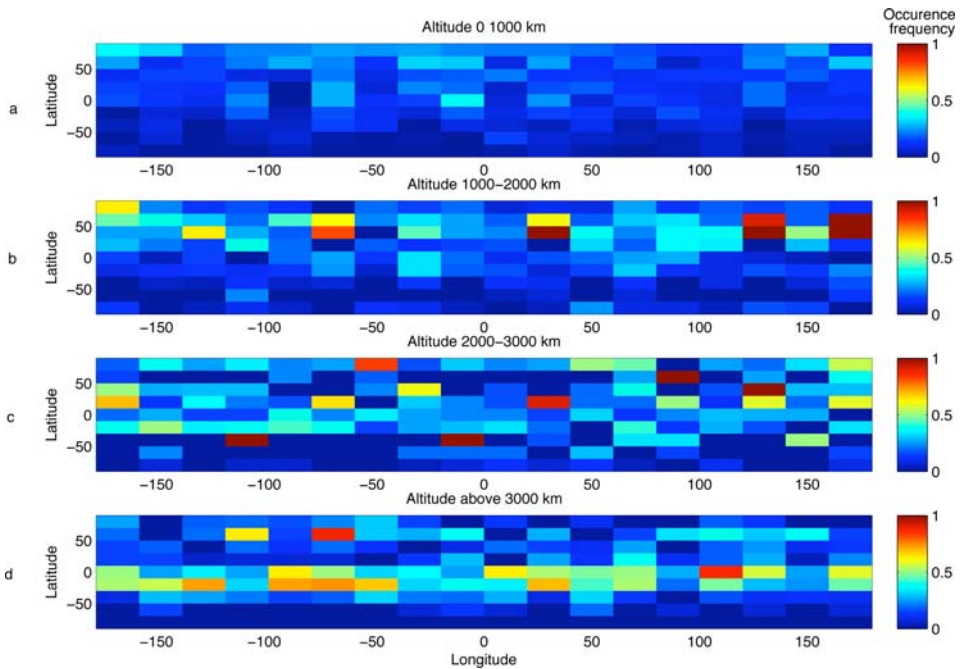


Figure 4. Distribution of occurrence rate of ions beams. Panel (a) shows the altitude interval up to 1000 km, (b) shows the interval 1000 to 2000 km, (c) 2000 to 3000 km and (d) 3000 up to 10000 km altitude.

southernmost latitudes at high altitude. Finally one may note that there is an increasing occurrence rate at higher altitude. As IMA cannot detect thermal ions this is consistent with an extended altitude range where ion energization is significant. This can be both thermal ionospheric origin ions and newly created pick-up ions.

One may also study the presence of ion beam events as a function of the magnetic field as determined from MGS statistics. We have used the data for 400 km altitude as provided by Connerney *et al.* (2001). Interpolating the MGS data (we used linear interpolation) at each measurement point yields rather few points above significant anomalies. We show in Figure 6 the occurrence frequency of ion beams for some altitude intervals as a function of radial magnetic field at 400 km altitude. Radial magnetic field was used because ion outflow can be expected along strong radial fields. Strong transverse fields can be expected to inhibit vertical plasma transport so we have made the same study with the transverse and total magnetic field as well, but with no significant differences in the result. Almost all data points are located above magnetic field values below 40 nT, as shown by the grey bars in the plot (number of data points on right y-axis). We can now discern an influence from magnetic anomalies on ion beams at the lowest altitudes. Up to 2000 km the likelihood of observing an ion beam decreases in the presence of even rather low

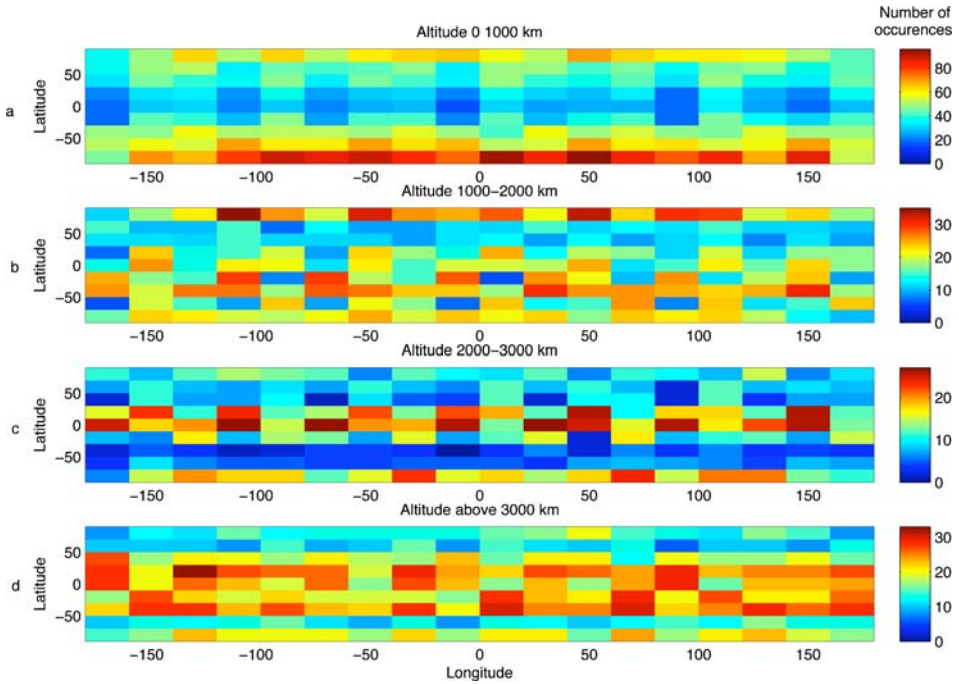


Figure 5. Distribution of number of different orbits of Mars Express passing through different latitude, longitude and altitude bins, when IMA was on in the right mode. Panel (a) shows the altitude interval up to 1000 km, (b) shows the interval 1000 to 2000 km, (c) 2000 to 3000 km and (d) 3000–10000 km altitude.

magnetic field strengths. The statistics are very poor for the data at higher magnetic field values, but there are a number of events there also for the lowest altitudes below 2000 km. In the altitude interval above 2000 km there is no influence on the occurrence of ion beams from the magnetic field for the values below 40 nT where statistics are relatively good. The north-south asymmetry seen in the latitude distribution could in principle cause a spurious dependence on the magnetic field as the magnetic fields are in general stronger in the southern hemisphere. We have therefore performed the same calculations for the southern hemisphere only but with no significant change in the result. The large scatter with some very high occurrence frequencies for higher magnetic field values is consistent with significant magnetic anomalies playing a particular role in some outflow events (like the field-aligned acceleration events reported by Lundin *et al.* (2006)) but the net contribution is small. We have made the same plot also for a magnetic map where we used the maximum magnetic field value within up to $\pm 5^\circ$ of each grid of the magnetic field map (which has a resolution of $1^\circ \times 1^\circ$) to allow for a less precise mapping to the closest strong anomaly. This caused a more even spread of the data and confirmed the lack of influence of magnetic fields on the large scale distribution for altitudes

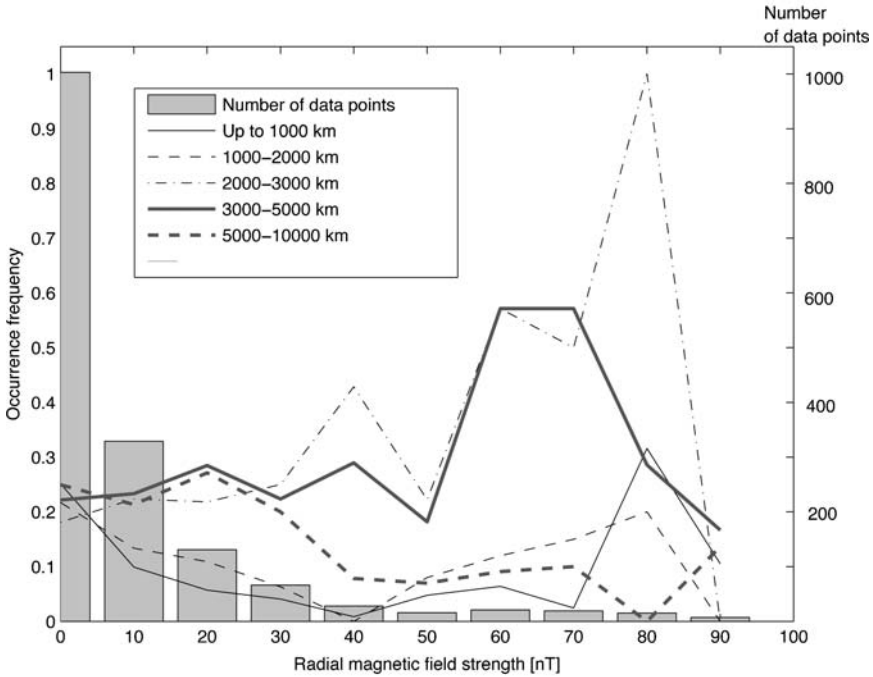


Figure 6. Occurrence rate of ions beams vs. radial crustal magnetic field at 400 km altitude below the spacecraft for 5 different altitude intervals as indicated in the figure. Grey bars in the background indicate the number of ion beam data points (summed over all altitude intervals) in each statistical bin.

above 2000 km. We also tried the transverse and total magnetic fields which resulted in somewhat larger scatter but otherwise little difference in the result. The “noisy” peaks for higher magnetic field values were most pronounced for the original radial magnetic field data used in Figure 6, indicating that these particular events indeed map rather precisely to the strong radial field regions.

We have in the discussion above used a radial mapping of the location of the spacecraft down to our reference magnetic field model at 400 km. The obvious alternatives are to compare to the magnetic field values of an extrapolated mathematical model (i.e. the Cain model) at the actual altitude of observation or do field-tracing along such a model, which must be coupled to an IMF/draped field-line model to justify the effort of such a precise mapping. The latter is desirable but outside the scope of our current work. We have tried the former but it suffers from the fact that all extrapolated model fields are weak at high altitudes whereas the radial field can be stretched out and therefore stronger during certain events. Relatively strong crustal fields at high altitude always correspond to strong crustal magnetic fields at low altitude as well.

3.4. DISTRIBUTION OF EVENTS WITH NO ENTRANCE DEFLECTION

The small data set from December 2005 to March 2006 (when IMA was run with entrance deflection off) is particularly important both because of its higher time resolution and its better ability to measure low energy ions. We have visually inspected all such orbits and picked out ion beam events in the lower altitude part. The heavy ion counts summed over all energies are plotted along the satellite track as shown in Figure 7 (background count levels subtracted). Also shown in Figure 7 is a grayscale map of the radial crustal magnetic field at 400 km altitude (Connerney *et al.*, 2001) so that the fine structure of the ion counts can be compared with the fine structure of the radial field. About half of the data points were obtained below 1500 km altitude, and altitudes up to 4000 km have been used. Clearly many of the events occur where there are no strong magnetic anomalies straight below the spacecraft. Fine structures also occur when no magnetic anomaly is nearby. A number of events with significant structure do occur close to magnetic anomalies, and the structure could possibly arise either from an interaction between pick-up

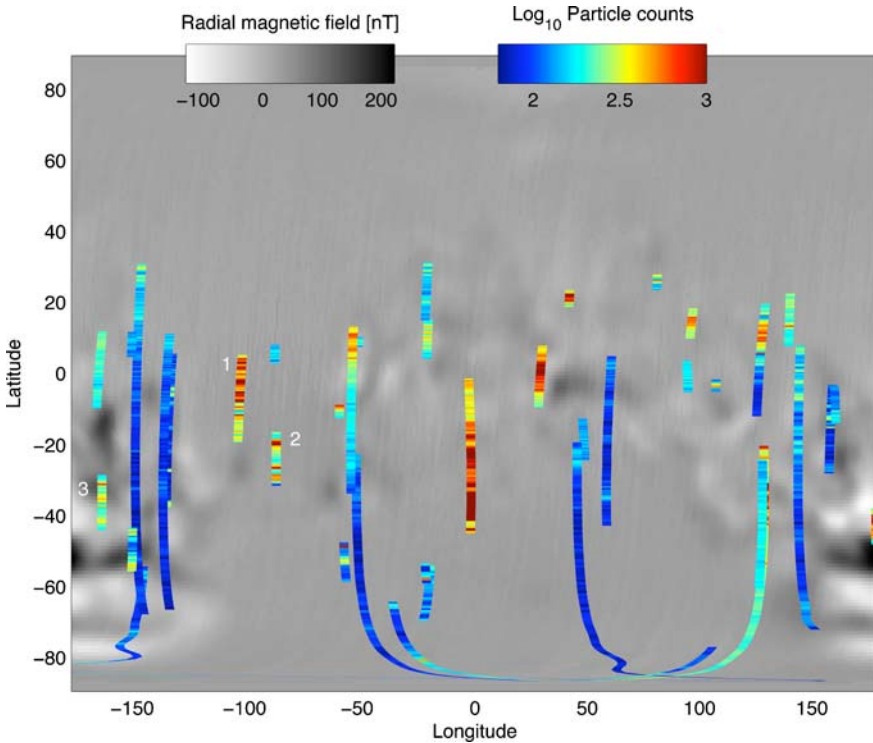


Figure 7. Counts in the heavy ion mass channels mapped radially to the planet, superposed on a map of the radial crustal field at 400 km as obtained from the MGS spacecraft. Three cases are marked with a number, these are discussed in more detail in the text.

ions and the anomalies or because the ions emanate from the anomalies as in the cases reported by Lundin *et al.* (2006). We leave a closer investigation of this to future case studies but show two sample cases here. The first, from 2006-02-16, numbered 2 in Figure 7, is a sample of a beam that appears very structured and occurs away from any anomaly, as shown in Figure 8. The other sample is shown in Figure 9 and was taken in the close proximity of a significant crustal magnetic anomaly. Both figures have four panels, where the first shows electron counts from the ELS electron spectrometer, the second shows proton counts, the third shows oxygen ion counts and the fourth shows altitude (black line, left y-axis) and radial magnetic field at 400 km altitude, interpolated from the statistical MGS results (red line, right y-axis). The oxygen ion counts dominated but may contain contributions from heavier ions (see Carlsson *et al.*, 2006, for details). Just as the impression one gets from the overview shown in Figure 7, there is indeed significant structure in the heavy ion counts in both cases. These are often correlated with variability

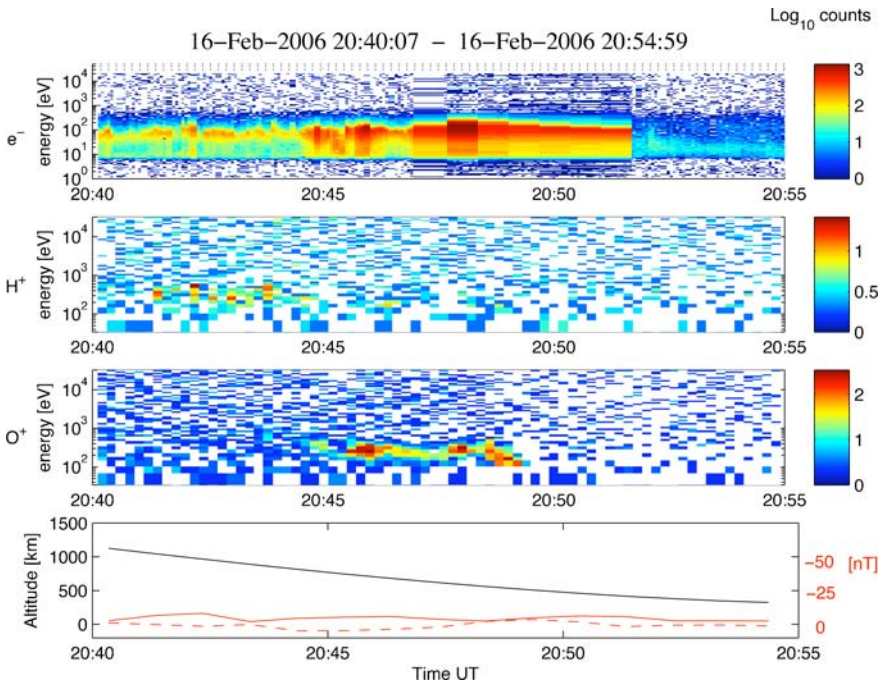


Figure 8. Sample energy spectra of a heavy ion beam from 2006-02-16 when no entrance deflection scanning was used. The first panel show the corresponding electron spectra summed over all sectors (the electrons are typically rather isotropic). The two consecutive panels show the H⁺ and O⁺ ion counts, summed over all sectors. Only a few sectors (of 22.5° × 5°) detect any ions at all. The Y-axis shows particle energy in eV for all of the first three panels, and the x-axis time (UT). The bottom panel shows the altitude of the spacecraft (black line, left y-axis [km]) together with the radial (red dashed line) and transverse (red solid line) magnetic field at 400 km altitude, radially below the spacecraft (right y-axis, [nT]).

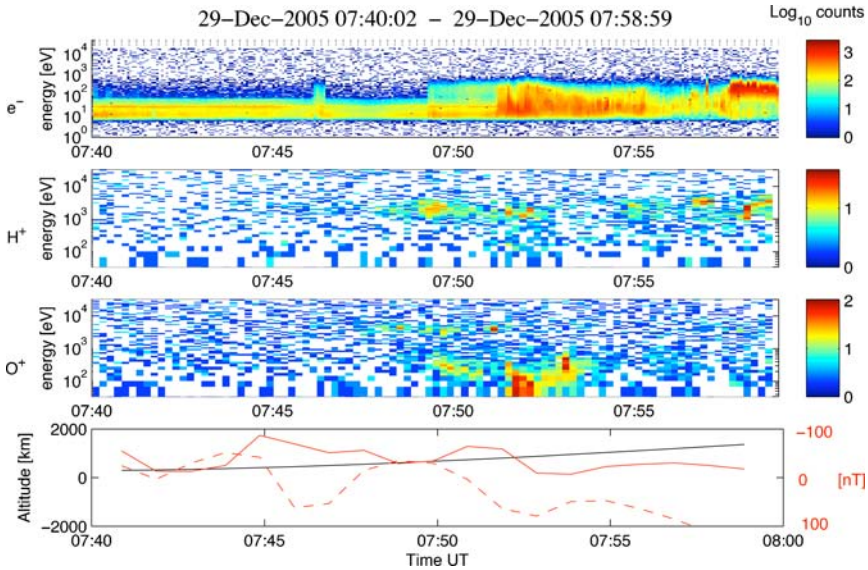


Figure 9. Sample energy spectra of a heavy ion beam from 2006-12-29 when no entrance deflection scanning was used. The first panel show the corresponding electron spectra summed over all sectors (the electrons are typically rather isotropic). The two consecutive panels show the H^+ and O^+ ion counts, summed over all sectors. Only a few sectors (of $22.5^\circ \times 5^\circ$) detect any ions at all. The Y-axis shows particle energy in eV for all of the first three panels, and the x-axis time (UT). The bottom panel shows the altitude of the spacecraft (black line, left y-axis [km]) together with the radial (red dashed line) and transverse (red solid line) magnetic field at 400 km altitude, radially below the spacecraft (right y-axis, [nT]).

in the electron counts but we leave the detailed comparison for future studies. In the case observed close to an anomaly it turns out that low energy ions are observed at a peak in the radial magnetic field (dashed red line). On both sides of the low energy ions we observe beams with a narrow energy distribution. Low energy ions are those most likely to be affected by the magnetic fields, and such low energy ionospheric ions are usually not observed in the ion beam events, (e.g. the samples shown in Figures 2 and 8). The low energy ions were not observed at the lowest point in the orbit, nor were low energy ions observed at the peak in the radial field which the spacecraft passed at a lower altitude at about 7:46 UT. The observed structure is therefore consistent with an influence due to the anomaly, but this is not a clear proof that this is really the case and anomalies are clearly not associated with such enhancements all the time. Rather the opposite is true according to our statistical results discussed in Section 3.3, where ion beams were less common above moderately strong (10–40 nT) crustal fields than over regions with the lowest crustal fields.

The most important observation is that the events occur everywhere regardless of the presence of anomalies and there is a considerable amount of fine structure

everywhere, not only close to anomalies. One may note that fine structure in the “no entrance deflection” cases can be due to flow direction changes, not necessarily a particle flux modulation, but it still represents a small scale structure in the plasma characteristics.

4. Discussion and Conclusions

The data shown in this paper clearly indicate that heavy ion beams (and thus of planetary origin) occur over most locations above Mars. This is a very expected result as planetary ions are expected to dominate in the magnetic pile-up region which is draped around the planet. There are, however, three interesting findings in our data set:

- (1) There is some north-south asymmetry in the data. Ion beams are somewhat less common at low altitudes (up to 1000) over the southern hemisphere and more common just below the equator in the southern hemisphere for high altitude (above 3000 km). North-south asymmetries are sensitive to orbit characteristics but the data we show have been normalized to take into account the number of observations in the different latitude-longitude-altitude intervals used in our study. There is no longitudinal variation resembling those of the magnetic anomalies. Our conclusion is that the latitudinal asymmetry is not directly caused by magnetic anomalies. One may have to compare with the average solar wind electric field direction and possibly planet rotation axis tilt to explain the difference. As was shown by Dubinin *et al.* (2005), Fedorov *et al.* (2005) the heavy ion flux distribution is well organized by the solar wind electric field. Furthermore the ion beam occurrence rate increases somewhat with altitude. This is consistent with an extended altitude region where ion energization up to the beam energies of 100 eV and above occurs.
- (2) A study of the dependence of ion beam occurrence rate vs. radial magnetic field at 400 km altitude revealed no dependence on ion beam occurrence at altitudes above 2000 km. For altitudes below 2000 km a dependence on ion beam occurrence could be seen. The occurrence frequency was highest for the lowest magnetic field region (0–10 nT) and decreased for the moderately strong crustal fields (about 40 nT). For higher magnetic field values the variability was large, mainly because of poor statistics but the decrease seen from about 0 to 40 nT magnetic field strength can clearly not be extrapolated to higher magnetic field cases. There was no signature of magnetic anomalies discernible in the longitude distribution of the ion beams, and the latitude asymmetry discussed above seems not to be directly related to magnetic anomalies. This is different from what is the case for electrons where the ionopause and magnetic-pileup boundary as detected from electron data are clearly modulated by the presence of magnetic anomalies (see references in introduction), and the strongest

fields have a clear and pronounced effect. Typical electron signatures associated with magnetic anomalies have been demonstrated (Mitchell *et al.*, 2001; Soobiah *et al.*, 2005). The reason for the discrepancy between ion and electron observations is most likely finite gyro radii effects of the ions for the energies observable by the IMA instrument. The beams observed by IMA typically have energies of several 100 eV. In a magnetic field of 50 nT a 300 eV O^+ ion has a gyro radius of 200 km. When the field is down to 10 nT the gyro radius is 1000 km. Therefore ions may be tied to the magnetic fields at low altitudes where the magnetic field is strong and the ion energy typically low. As the ions gain energy they will still be affected by magnetic anomalies, but in a dynamical way, they will not stay in place the way the electrons do. The ions may be accelerated along the field-line, in which case the mirror force will keep the outflowing ions beam-like and tied to the original field-line (Lundin *et al.*, 2006) which is indeed the only clear ion-magnetic anomaly association reported). The influence may also be through small scale ripples in the draped field-lines, causing non-adiabatic drift and acceleration through the centrifugal force mechanism (Cladis, 1986; Cladis *et al.*, 2000).

It could, despite gyro-radius considerations, be possible that the actual number flux and ion composition would be influenced by magnetic anomalies. This would then mainly concern ionospheric upflow and escape, not pick-up ions. At Earth the ionospheric escape is a two-stage process consisting of initial upflow in the ionosphere observable for example by incoherent scatter radar [e.g. (Nilsson *et al.*, 1996; Ogawa *et al.*, 2003)] and subsequent energization to escape velocity at higher altitudes. The initial upflowing ions are typically gravitationally bound and flow down again unless further heating processes take place at higher altitudes (as is the case at Earth, from the topside ionosphere and throughout the magnetosphere, e.g. see discussion and references in Nilsson *et al.* (2004)). The lower altitude processes regulate the number flux of planetary origin ions and, if something similar occurs at Mars, would most likely be strongly affected by the magnetic anomalies as these regulate ionospheric scale height and heating rates [e.g. (Krymskii *et al.*, 2003)]. A possible explanation for our results of decreasing ion beam occurrence for intermediate strength crustal fields is that most field-lines close below the spacecraft and reduce the vertical transport of ionospheric ions. It would therefore be worthwhile to study the number flux and detailed composition of the planetary origin fluxes as a function of geographic location above Mars. This is, however, a rather demanding task as the detailed ion composition requires a manual inspection of every mass spectrogram [e.g. (Carlsson *et al.*, 2006)] and is thus beyond the scope of this report.

- (3) There is considerable small scale structure in many of the ion beams observed. Some of these structures may indeed be caused by magnetic anomalies which show variations on the proper spatial scale. It would be of interest from a fundamental plasma physics point-of-view to identify some such cases and study

them in detail, but if magnetic anomalies disperse or further energize already picked-up ions passing through them this should not be of major importance for the total outflow. Outflow caused more directly by processes associated with the crustal fields could have some influence on the total outflow. If that is the cause of small scale structures then due to the small size it cannot have a large overall impact on the ion escape from Mars. Inhibition of vertical transport and therefore lower escape is rather more in line with the results obtained in this study (see point 2 above). The data we presented in Figure 7 contained cases with considerable fine structure also when no magnetic anomalies were nearby so clearly there are other plasma structuring processes at work as well.

Acknowledgments

This project was supported by the Swedish National Space Board and the funding agencies of our co-investigators. The MGS magnetic field data was downloaded from the Goddard Space Flight Center web pages, and we gratefully acknowledge the work of GSFC, JPL and all other institutes and individuals involved in the Mars Global Surveyor MAG-ER experiment.

References

- Acuña, M. H., Connerney, J. E. P., Wasilewski, P., Lin, R. P., Anderson, K. A., Carlson, C. W., *et al.*: 1998, *Science* **279**(5357), 1676, doi: 10.1126/science.279.5357.1676.
- Barabash, S.: 2006, *Plan Space Sci.*, submitted.
- Barabash, S., Dubinin, E., Pisarenko, N., Lundin, R., and Russell, C.: 1991, *Geophys. Res. Lett.* **18**, 1805.
- Bertucci, C., Mazelle, C., Acuña, M., Russel, C., and Slavin, J.: 2005, *J. Geophys. Res.* **110**(A01209), doi: 10.1029/2004JA010,592.
- Brain, D., Halekas, J. S., Lillis, R., Mitchell, D., Lin, R., and Crider, D.: 2005, *Geophys. Res. Lett.* **32**, doi: 10.1029/2005GL023,126.
- Brain, D., Halekas, J. S., Peticolas, L., Lin, R., Luhmann, J., Mitchell, D., *et al.*: 2006, *Geophys. Res. Lett.* **33**(L01201), doi: 10.1029/2005GL024,782.
- Breus, T., Krymskii, A., Lundin, R., Dubinin, E., Luhmann, J., Yeroshenko, Y., *et al.*: 1991, *J. Geophys. Res.* **96**(A7), 11165–11174.
- Cain, J., Ferguson, B. B., and Mozzoni, D.: 2003, *J. geophys. Res.* **108**(E2), doi 10.1029/2000JE001, 487.
- Carlsson, E., Fedorov, A., Barabash, S., Budnik, E., Grigoriev, A., Gunell, H., *et al.*: 2006, *Icarus*, **182**(2), 320.
- Cladis, J. B.: 1986, *J. Geophys. Res.* **13**, 893.
- Cladis, J. B., Collin, H. L., Lennartsson, O. W., Moore, T. E., Peterson, W. K., and Russell, C. T.: 2000, *Geophys. Res. Lett.* **27**, 915, doi: 10.1029/1999GL10737.
- Connerney, J. E. P., Acuna, M. H., Wasilewski, P. J., Ness, N. F., Réme, H., Mazelle, C., *et al.*: 1999, *Science* **284**(5415), 794.

- Connerney, J. E. P., Acuna, M. H., Wasilewski, P. J., Kletetschka, G., Ness, N. F., Réme, H., *et al.*: 2001, *Geophys. Res. Lett.* **28**(21), 4015.
- Crider, D., Cloutier, P., Law, C., Walker, P., Chen, Y., Acuña, M., *et al.*: 2000, *Geophys. Res. Lett.* **27**(1), 45.
- Crider, D., Acuña, M., Connerney, J., Vignes, D., Ness, N., Krymskii, A., *et al.*: 2002, *Geophys. Res. Lett.* **29**(8), doi: 10.1029/2001GL013,860.
- Dubinin, E., Lundin, R., Fränz, M., Woch, J., Barabash, S., Fedorov, A., *et al.*: 2006, *Icarus*, **182**(2), 337.
- Fedorov, A., Budnik, E., Sauvaud, J. A., Mazelle, C., Barabash, S., Lundin, R., *et al.*: 2006, *Icarus*, **182**(2), 329.
- Fränz, M., Winningham, J., Dubinin, E., Roussos, E., Woch, J., Barabash, S., *et al.*: 2006, *Icarus*, **182**(2), 406, doi: 10.1016/j.icarus.2005.11.016.
- Krymskii, A., Breus, T., Ness, N., Hinson, D., and Bojkov, D.: 2003, *J. Geophys. Res.* **108**(A12), doi: 10.1029/2002JA009,662.
- Lundin, R., Zakharov, A., Pellinen, R., Hultqvist, B., Borg, H., Dubinin, E., *et al.*: 1989, *Nature* **341**, 609.
- Lundin, R., Dubinin, E. M., Koskinen, H., Norberg, O., Pissarenko, and N., Barabash, S. W.: 1991, *Geophys. Res. Lett.* **18**(6), 1059.
- Lundin, R., Barabash, S., Andersson, H., Holmström, H., Grigoriev, A., Yamauchi, M., *et al.*: 2004, *Science* **305**, 1933.
- Lundin, R., Winningham, D., Barabash, S., Frahm, R., Andersson, H., Holmström, M., *et al.*: 2006, *Icarus*, **182**(2), 308, doi: 10.1016/j.icarus.2005.10.035.
- Lundin, R., Winningham, D., Barabash, S., Frahm, R., Holmström, M., Sauvaud, J. A., *et al.*: 2006, *Science* **311**(5763), 980.
- Mitchell, D., Lin, R., Rème, H., Crider, D., Cloutier, P., Connerney, J., *et al.*: 2000, *Geophys. Res. Lett.* **27**(13), 1871.
- Mitchell, D., Lin, R., Mazelle, C., Rème, H., Cloutier, P., Connerney, J., *et al.*: 2001, *J. Geophys. Res.* **106**(E10), 23419.
- Nagy, A., Winterhalter, D., Sauer, K., Cravens, T., Brecht, S., Mazelle, C., *et al.*: 2004, *Space Sci. Rev.* **111**(1–2), doi: 10.1023/B:SPAC.0000032,718.47,512.92.
- Ness, N., Acuña, M., Connerney, J., Kliore, A., Breus, T., Krymskii, A., *et al.*: 2000, *J. Geophys. Res.* **105**(A7), 15991.
- Nilsson, H., Yamauchi, M., Eliasson, L., Norberg, O., and Clemmons, J.: 1996, *J. Geophys. Res.* **101**, 10947.
- Nilsson, H., Joko, S., Lundin, R., Réme, H., Sauvaud, J. A., Dandouras, I., *et al.*: 2004, *Ann. Geophys.* **22**, 2497.
- Nilsson, H., Lundin, R., Lundin, K., Barabash, S., Borg, H., Norberg, O., *et al.*: 2006, *Space Sci. Rev.*, doi: 10.1007/s11214-006-9031-z.
- Ogawa, Y., Fujii, R., Buchert, S. C., Nozawa, S., and Ohtani, S.: 2003, *J. Geophys. Res.* **108**, doi: 10.1029/2002JA009,590.
- Soobiah, Y., Coates, A., Linder, D., Kataria, D., Winningham, J., Frahm, R., *et al.*: 2006, *Icarus*, **182**(2), 396, doi: 10.1016/j.icarus.2005.10.034.
- Trotignon, J., Dubinin, E., Réjan, G., Barabash, S., and Lundin, R.: 1996, *J. Geophys. Res.* **101**(A11), 24965.
- Trotignon, J. G., Mazelle, C., Bertucci, C., and Acuna, M. H.: 2006, *Plan Space Sci.* **54**, 357.
- Vignes, D., Mazelle, C., Réme, H., Acuña, M., Connerney, J., Lin, R., *et al.*: 2000, *Geophys. Res. Lett.* **27**(1), 49.
- Winningham, J., Frahm, R., Sharber, J., Coates, A., Linder, D., Soobiah, Y., *et al.*: 2006, *Icarus*, **182**(2), 360, doi: 10.1016/j.icarus.2005.10.033.